An analysis of the potential water loss through the humid streams leaving PEM-type electrolyzers

Raghuvaran Ganesan

Dubai, United Arab Emirates

Antonio Atienza Márquez

Multiphysics Modelling School, University of Malaga, Spain

Juan Manuel Paz

Multiphysics Modelling School, University of Malaga, Spain

Abstract. Proton Exchange Membrane (PEM) based water electrolyzers play a pivotal role in hydrogen production, which is necessary for an efficient energy mix in the future. Green hydrogen production is achieved through water electrolysis, which demands a large supply of high-purity water. Water losses through humid streams are evaluated using fundamental principles through this modeling study under operational conditions of typical PEM water electrolyzers. It is revealed that the water transport through PEM on the cathode H_2 side is affected by transport properties in the anode domain as well as the operating conditions, i.e., the V-I characteristics of the system. The water flux through the H_2 side of the PEM in a water electrolyzer is estimated to be 0.035 g/(cm^2·min) when operating at nearly 2.4 A/cm^2 at 2.2V applied across the cell. This accounts for a potential water loss of nearly 26% of the theoretical water consumption at the anode.

I. INTRODUCTION

Electrolysis of water is considered a primary technology for green hydrogen production with the lowest carbon footprint [1]. Water electrolyzers based on Proton Exchange Membrane (PEM) are promising systems characterized by the ability for technological commercialization, quick response, and the ability to operate at high current densities (1-2 A/cm^2), delivering high-purity gas from compactly designed systems. Compared with other electrolyzers like alkaline water electrolyzers, PEM electrolyzers allow operation at higher current densities, which is a key factor in achieving power efficiency and higher throughput.

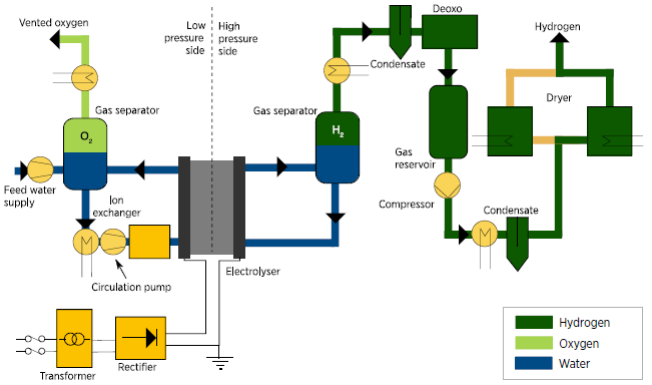

FIG. 1. Typical system design for a PEM Electrolyzer [2]

Industrial-scale PEM water electrolyzers are typically operated at 30–40 bar hydrogen outlet pressures, sometimes reaching as high as 70 bar. However, operations at higher pressures are desirable based on downstream applications, *viz.* injection into natural gas storage, other syntheses like green methanol/ammonia production, etc. [4],[5].

PEM electrolyzers typically operate with a relatively higher cell pressure under 70 bar at an operating temperature of 30-80 °C, achieving an overall efficiency of 50-83% [1],[3]. Despite the higher efficiency and gas purity, this approach typically incurs 2 to 4 times the average cost per kg of H_2 gas compared to other technologies [1],[2]. In the case of unbalanced electrolyzer configurations, the typical anode side pressures are in the range of 0.8–1.3 bar [5].

Green hydrogen production is achievable when energy from green sources is used. For the effective long-term life of PEM electrolyzers, it is essential to ensure the availability of high-purity water as the cathode catalyst layers and the proton exchange membrane used are sensitive to contaminants[14]. Thus, water management is one of the key driving factors in successfully implementing climate-friendly water electrolyzers with an adequately extended lifetime, thereby reducing the net carbon footprint.

The effect of water drag across the membrane is suspected to be a potential means of losing high-purity water in the circuit. Mechanism and effects of water drag across the PEM are widely reported in the context of PEMFCs, considering it a threat to the reduction in active surface area available for ionic interactions at the electrodes under flooded conditions. The effect of water transport across the PEM and the extent of potential water losses in a PEM-based water electrolyzer under typical operating conditions are studied and reported with emphasis on the effect of water inlet velocity at the anode side.

II. MATERIALS AND METHODS

A water electrolyzer is an electrochemical cell that produces hydrogen gas by electrolysis (dissociation) of water. Water molecules are oxidized at the anode, generating O_2 gas

and protons (H^+ ions), which migrate through the electrolyte, i.e., the Proton-exchange Membrane. Meanwhile, the external power source releases electrons in the electronic pathway. The protons reaching the cathode are reduced to H_2 gas. The working principle of a PEM-based Water Electrolyzer is shown in FIG. 2.

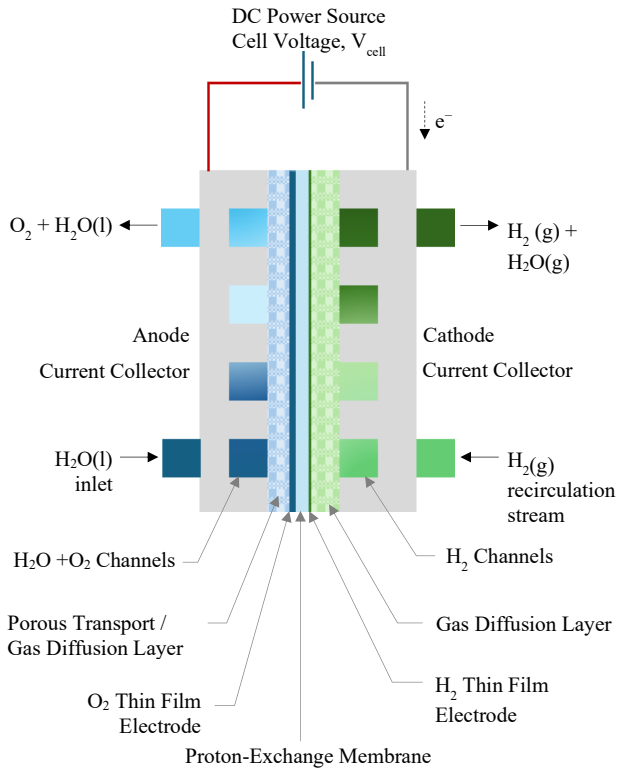

FIG. 2. Working Principle of a PEM Electrolyzer Module

A closer view of the sandwiched assembly with details of the diffusion layers, electrodes with active catalysts, and the Membrane is shown in FIG. 3.

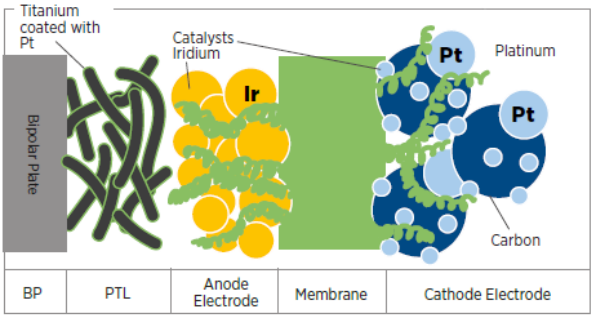

FIG. 3. Cell-level view of a PEM Electrolyzer [2]

A model is built, as shown in FIG. 4 based on the system description as a fully parameterized geometry. The geometry consists of the following layers on either side of the PEM water electrolyzer stack:

- gas flow channel (domain)
- current collector (boundary)
- gas diffusion layer / porous transport layer (domain)
- thin film electrode boundary (boundary)
- Proton-Exchange Membrane (domain)

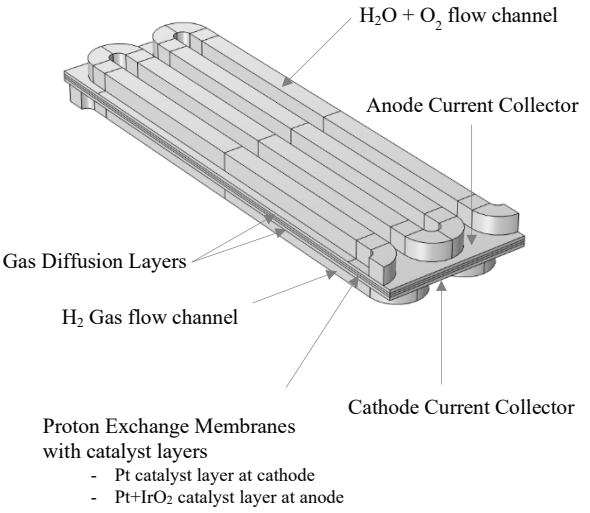

FIG. 4. Geometry of PEM Water Electrolyzer Element

For computational modeling, the geometric characteristics of the model are chosen as detailed in Table 1. The plate length results from the number of passes considered in the etched flow channels. The geometry represents nearly 50% of the typical electrode surface used in experiments by M. K. Debe *et al.* [10]. The geometry is constructed with half membrane thickness on the anode side and formed as a geometric union. Subsequently, the anode domain is mirrored and rotated to form the cathode sides. The anode and cathode domains are then assembled with an identity pair at the boundary formed at the center of the PEM. Forming assembly pairs facilitates better flexibility in mesh generation for handling physical changes across the anode and cathode domains.

The domain shown as Proton Exchange Membrane is assigned as *Nafion®, EW 1100, Liquid Equilibrated, Protonated* from the COMSOL material library. Properties of species (H_2, O_2, and H_2O) are handled by the module. The electrical conductivity of diffusion electrodes and porosity and permeability of the diffusion/transport layers are fed as parameters based on assumptions and default values, which will be further detailed in subsequent sections.

Table 1. Geometric Characteristics of the PEM electrolyzer model

Parameter	**PEM Electrolyzer**
Plate width	20 mm
Plate length	3 mm

Parameter	PEM Electrolyzer
Channel width	0.8 mm
Channel height	0.8 mm
Channel rib width	0.7mm
Number of channel passes	4 on either side (2 pairs)
Total PEM thickness	178 µm [9],[10]
Gas diffusion layer / porous transport layer thickness	140 µm [9],[10] on either side
Anode catalyst layer ($Pt+IrO_2$) thickness	30 µm [9],[10]
Cathode catalyst layer (Pt) thickness	10 µm [9],[10]
Active Specific Surface Area	$1x10^7$ (m^2/m^3) for the Pt catalyst layer $1x10^8$ (m^2/m^3) for Pt/IrO_2 catalyst layer *(assumed)*

This study is carried out using the *Water Electrolyzer* module available in *COMSOL 6.3*, which is a sophisticated physics interface developed for addressing current distribution characteristics in electrochemical systems with consideration to chemical species transport features in tandem with heat and mass transport phenomena influenced by fluid dynamics through porous and non-porous electrodes. The water electrolyzer module supports momentum transport, considering Darcy's flow. For a more flexible exploitation of the transport properties in the flow channels and diffusion layers, the *Free and Porous Medium Flow* module is used for the flow channels and diffusion layers on both the anode and cathode sides. This approach can allow for turbulent and non-darcian transport phenomena through a porous medium when intended. The *Water Electrolyzer* module fetches the pressure, velocity fields, and other mass transport properties from the respective *Free and Porous Medium Flow* modules through the *Reacting Flow, H_2 Gas Phase,* and *Reacting Flow, and O_2 Gas Phase* nodes implemented through the *Multiphysics* node.

When building the geometry, selections were included to control the mesh development. Quadratic mesh elements were developed for regular and straight surfaces and swept through the domains, whereas triangular mesh elements were generated on surfaces with curvature and corner features. Boundary layers were implemented at interfaces between the gas flow channels and the diffusion layers. The resulting mesh in various domains is shown in FIG. 5.

The study of the model is conceived with steps in a specific order to provide sequential outputs to optimize the subsequent step, thereby facilitating better convergence. The first step in the study is Current Distribution Initialization based on *primary current distribution*, considering ohmic currents, followed by a second Current Distribution Initialization based on *secondary current distribution*, accounting for the polarization effects and corrections of reversible voltages based on operating temperatures. The third step solves for pressure and velocity properties in the anode domain coupled with the water electrolyzer node. The reacting flow node was not activated during this step of the study. The fourth step takes a similar approach on the cathode side. The final step is the fully activated study step, which solves for potentials and transport properties through the reacting flow nodes.

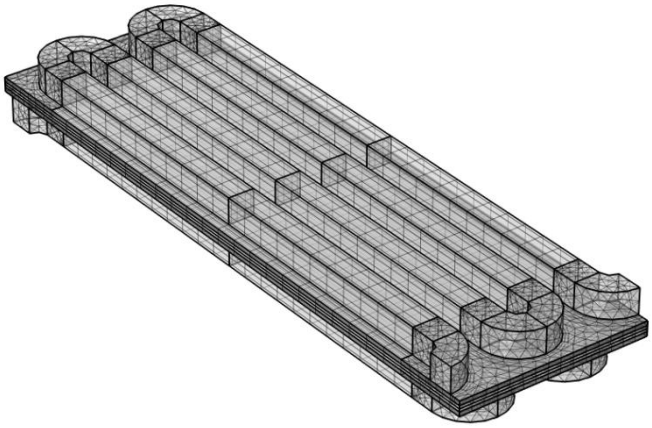

FIG. 5. Meshing of PEM Electrolyzer Model

Similar to simulation studies by A. S. Tijani et al. [9] based on the works of M. K. Debe et al. [10], an interpolation function *i_exp (t)* is defined as shown in FIG. 6 for comparison of modeling outcomes against the experimental data (Note: '*t*' is a default help variable in this context to represent applied cell voltage measured in volts).

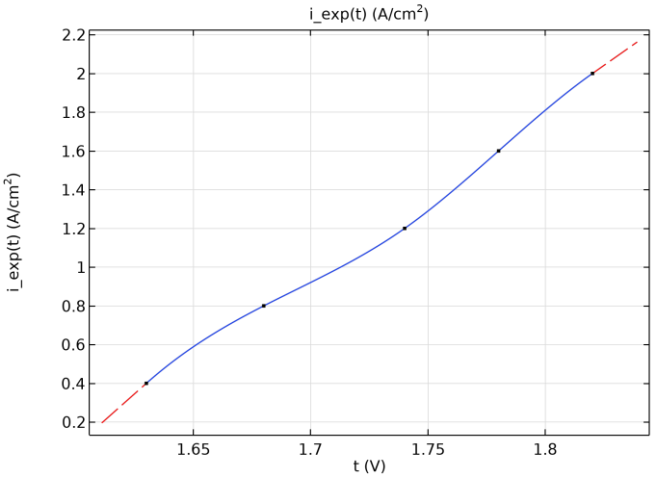

FIG. 6. Experimental data [9],[10]

However, the exact experimental conditions could not be retrieved from the available information, and assumptions have been made about several parameters that influence the overpotentials and the cell voltages.

Boundary Probes are defined at the cathode (H_2 side) electrode/electrolyte interface to evaluate the average local current density associated with the hydrogen evolution reaction. It is to be noted that the boundary is a 2D geometry and needs to be corrected for the active surface area and catalyst thickness layers applicable for the porous electrode to convert the results to appropriate scales. Similar boundary probes were also defined to evaluate the activity of water and the water flux through the cathode side of the *Membrane*, i.e., the same boundary element as the *Thin H_2 Gas Diffusion Electrode* node.

Four cases were chosen for a detailed analysis:

- **Case 1** considers neither the velocity fields in domains nor the membrane crossover due to electroosmotic water drag.
- **Case 2** considers water crossover through the membrane due to electroosmotic water drag, yet in the absence of velocity fields.
- **Case 3** considers the effects of velocity fields on water crossover through the membrane due to electroosmotic water drag
- **Case 4** considers the effects of velocity fields, assuming water does not cross through the membrane.

All studies were conducted as *stationary* studies. Cell voltage was swept from 1.3V to 2.2V using the auxiliary sweep node in Step 5.

III. THEORY

The *Water Electrolyzer* module solves the physics for four dependent variables: electrolyte potential (ϕ_l) and electric potential (ϕ_s) by default. Optional dependent variables such as chemical potential ($\mu_{0,i}$) and mass fractions (ω_i) of species involved are solved when additional species (e.g., H_2O) are selected in the gas mixture and when gas phase diffusion options are respectively activated.

A. Electrochemical Model

The equations defining the conservation of charges in electronic and electrolytic media are given by [19],

$$\nabla \cdot i_l = i_{v,total} \tag{1}$$

$$i_l = -\sigma_{l,eff} \nabla \phi_l \tag{2}$$

$$\nabla \cdot i_s = -i_{v,total} \tag{3}$$

$$i_s = -\sigma_s \nabla \phi_s \tag{4}$$

where $i_{v,\ total}$ is the volumetric current density contribution from the porous electrodes, while i_l and i_s are the local current densities in the electrolytic and electronic phases, respectively. At the same time, ϕ_l and ϕ_s are the corresponding electrolyte potential and electric potentials.

The effective conductivity ($\sigma_{i,eff}$) is applicable in the electrolytic phase and is a function of several parameters, including water activity, water absorption and other transport mechanisms related to species active in the PEM. The electronic conductivity (σ_s) is a characteristic property of the electronically conducting medium and is assumed to be isotropic. Usually, electronic conductivity is affected by temperature; however, it is negligible in the given operating conditions.

The cell voltage (V_{cell}) is applied as Dirichlet boundary conditions at the anode current collector boundary. The cathode current collected is assigned as the electric ground, which is also a Dirichlet boundary condition setting the electric potential(ϕ_s) to 0V. An expression for current density is thus required to solve the electric potential in the electronically conducting phases using Ohm's law based on the conductivity (σ_s) of the respective medium.

B. Electrolytic Current Distribution

The electrolyte potential (ϕ_l) is solved using the electrode kinetics defined based on the concentration-dependent Butler-Volmer equation given by the following expression at the respective electrodes[19].

At the cathode for the hydrogen evolution reaction (HER),

$$i_c = i_{0,ref,HER}\left(\frac{p_{H_2}}{p_{cell}} exp\left(\frac{\alpha_{a,c}F}{RT}\eta_c\right) - exp\left(\frac{\alpha_{c,c}F}{RT}\eta_c\right)\right) \tag{5}$$

At the anode for the oxygen evolution reaction (OER),

$$i_a = i_{0,ref,OER}\left(\left(\frac{p_{O_2}}{P_{cell}}\right)^{\frac{1}{2}} exp\left(\frac{\alpha_{a,a}F}{RT}\eta_a\right) - \frac{p_{H_2O}}{P_{cell}} exp\left(\frac{\alpha_{a,c}F}{RT}\eta_c\right)\right) \tag{6}$$

At standard temperatures and pressures, the decomposition of water occurs at 1.23V at the anode boundary, which is usually referred to as the *reversible voltage* (V^0_{rev} or E^0_{rev})[14]. This voltage is dependent on the operating temperature and pressure given by Equation 7[14],[19],

$$E_{rev} = E^0_{rev} + \frac{RT}{2F}\ln\left(\frac{P_{H_2}\,P_{O_2}^{\frac{1}{2}}}{P_{H_2O}}\right) \quad (7)$$

Thus, the overall constituents of cell voltage (V_{cell}) can be given by [14]–[15][19]

$$V_{cell} = E_{rev} + \phi_s + \phi_l + \eta_{act} + \eta_{it} \quad (8)$$

where ϕ_s and ϕ_l are the ohmic voltage losses related to the conductivity of the electrode and electrolyte domains respectively, while η_{act} is the overpotential related to activation of electrode reactions at the electrolyte-interface and η_{it} is the overpotential related to the work done in transfer of reacting species from the bulk to the electrode-electrolyte interface.

C. Gas Phase Diffusion – Transport Model

When gas phase diffusion is included, the multicomponent gas phase mass transport is modeled using Maxwell–Stefan's equations in equations (5) to (8).

$$\nabla \cdot j_i + \rho(u \cdot \nabla)\omega_i = R_{i,total} \quad (9)$$

$$j_i = -\rho\omega_i \sum_k \widetilde{D}_{ik,eff}\,\boldsymbol{d}_k \quad (10)$$

$$\boldsymbol{d_k} = \nabla x_k + \frac{1}{P_A}[(x_k - \omega_k)\nabla P_A] \quad (11)$$

$$x_k = \frac{\omega_k}{M_k} M_n \quad (12)$$

$$D_{ik,eff} = \epsilon_g^{1.5} D_{ik} \quad (13)$$

where mass average density (j_i) is given as a function of density (ρ), velocity (u), mass fractions (ω), diffusion driving force ($\boldsymbol{d_k}$), absolute pressure (P_A) and its local gradient, mole fractions (x_k), species-specific molar mass (M_k), mean molar mass (M_n) and the reaction term (R_i). The effective diffusivity ($D_{ik,\,eff}$) for the respective species is approximated using the Bruggerman correction for porous domains given by Equation 13 based on the gas pore volume fraction (ϵ_g).

The thin film electrode node then contributes to solving for the electrolyte potential (ϕ_l) by evaluation of local current densities (i_l). It is based on the system of equations given by Equations 14 to 18.

$$\mathbf{n} \cdot i_l = d_{gde}\left(\sum_m i_{v,m} + i_{v,dl}\right) \quad (14)$$

$$\mathbf{n} \cdot i_s = -d_{gde}\left(\sum_m i_{v,m} + i_{v,dl}\right) \quad (15)$$

$$-\mathbf{n} \cdot (j_i + \rho u_s \omega_i \boldsymbol{n}) = d_{gde}\sum_m R_{i,m} \quad (16)$$

$$\rho u_s = \mathbf{n} \cdot \sum_i (j_i + \rho u_s \omega_i \boldsymbol{n}) \quad (17)$$

$$-\boldsymbol{n} \cdot \rho\boldsymbol{u} = d_{gde}\sum_i\sum_m R_{i,m} \quad (18)$$

From the equations, it can be seen that the mass fractions (ω_i), reaction term (R_i), and Stefan velocity (u_s) are terms that need to be determined to facilitate the solution to electrolyte potentials. In this study, the pressure (p) and velocity vector ($\boldsymbol{u}$) in the gas channel and the gas diffusion / porous transport layer are solved through *Free and Porous Medium Flow* modules using the system of equations given by Equations 19 to 21 for free flow through channels and Equations 22 to 23 for flow through porous domains.

$$\rho(\boldsymbol{u} \cdot \nabla)\boldsymbol{u} = \nabla \cdot [-p\boldsymbol{I} + \boldsymbol{K}] + \boldsymbol{F} \quad (19)$$

$$\boldsymbol{K} = \mu(\nabla\boldsymbol{u} + (\nabla\boldsymbol{u})^T) \quad (20)$$

$$\rho\nabla \cdot \boldsymbol{u} = 0 \quad (21)$$

$$\frac{1}{\epsilon_p}\rho(\boldsymbol{u} \cdot \nabla)\boldsymbol{u}\frac{1}{\epsilon_p} = \nabla \cdot [-p\boldsymbol{I} + \boldsymbol{K}] - \left(\mu\kappa^{-1} + \beta\rho|\boldsymbol{u}| + \frac{Q_m}{\epsilon_p^2}\right)\boldsymbol{u} + \boldsymbol{F} \quad (22)$$

$$\rho\nabla \cdot \boldsymbol{u} = Q_m \quad (23)$$

$$\boldsymbol{K} = \mu\frac{1}{\epsilon_p}(\nabla\boldsymbol{u} + (\nabla\boldsymbol{u})^T) - \frac{2}{3}\mu\frac{1}{\epsilon_p}(\nabla \cdot \boldsymbol{u})\boldsymbol{I} \quad (24)$$

where $\boldsymbol{K}$ is the viscous stress tensor, $\boldsymbol{F}$ is the volume force, μ is the dynamic viscosity, ϵ_p is the porosity, κ is the medium's permeability, Q_m is the source term, and $\boldsymbol{I}$ is the inertial force(s). The fluid on the anode side is predominantly water and hence considered incomprehensible under typical operating conditions. In contrast, the fluid on the cathode side is predominantly H_2 gas, potentially with traces of water vapor, and hence considered compressible flow.

Based on the resolved pressure and velocity fields from the respective *Free and Porous Medium Flow* modules for the anode and cathode domains, the *Reacting flow* module assigned to the respective domains under the *Multiphysics* node contributes the necessary inputs for the Water The

electrolyzer module, namely the source term (Q_m), is given by Equation 25, and Stefan velocity (u_s) is given by Equation 17.

$$Q_m = \sum_i R_i \tag{25}$$

D. Membrane Transport Model

A transport model for the movement of water based on mass and charge conservation through both liquid-equilibrated and vapor-equilibrated PEM was developed by Weber and Neumann [12] for PEM/water systems incorporating elements to address Schröder's Paradox: the tendency of PEM in a PEM/Water system to absorb significantly more water when in contact with a liquid phase than from a similar contact with a vapor phase, despite the same chemical potential of water.

Considerations for water transport through PEM can be modeled in water electrolyzers based on the *Electroosmotic Water Drag Theory*[19]. *The membrane* node of the *Water Electrolyzer* module uses the equations given by Equations 26 to 31 to solve the membrane water transport due to electroosmotic drag (EOD) and pressure gradients across the Membrane.

$$i_l = -\sigma_{pem}\nabla\phi_l - \frac{\sigma_l \xi}{F}\nabla\mu_0 \tag{26}$$

$$\nabla \cdot i_l = 0 \tag{27}$$

$$N_{H_2O} = \frac{\sigma_{pem}\xi}{F}\nabla\phi_l + \left(\alpha_{wtc} + \frac{\sigma_{pem}\xi^2}{F^2}\right)\nabla\mu_0 \tag{28}$$

$$\nabla \cdot N_{H_2O} = 0 \tag{29}$$

$$\nabla\mu_0 = RT\nabla\ln(a_0) + V_{H_2O}\nabla p_{H_2O(l)} \tag{30}$$

$$V_{H_2O} = {}^{M_{H_2O}}/_{\rho_{H_2O}} \tag{31}$$

where N_{H_2O} is the water flux through PEM, ξ is the electroosmotic coefficient, α_{wtc} is the water transport coefficient, σ_{pem} is the ion conductivity of PEM/water system, a_0 is the thermodynamic activity of water (=1 for liquid equilibrated membrane), V_{H_2O} is the partial molar volume, M_{H_2O} is the molar mass and p_{H_2O} is the partial pressure of water.

At the H_2 gas phase boundary with the cathode gas diffusion electrode, the liquid-equilibrated Membrane is expected to exhibit absorption-desorption characteristics similar to those of a vapor-equilibrated Membrane. This consideration is implemented using Equations 32 to 34, leading to the momentum transfer equation and Stefan velocity specific to water transport through PEM, given by Equations 35 and 36, respectively.

$$-\boldsymbol{n}\cdot N_{H_2O} = r_{abs,dsp} \tag{32}$$

$$r_{abs,dsp} = k_{abs,dsp}\left(\frac{p_{H_2O(g)}}{p_g^0} - a_0\right) \tag{33}$$

$$\boldsymbol{n}\cdot\left(j_{H_2O} + \rho u_s \omega_{H_2O}\boldsymbol{n}\right) = -M_{H_2O}\, r_{abs,dsp} \tag{34}$$

$$\boldsymbol{n}\cdot\rho u = -M_{H_2O}\, r_{abs,dsp} \tag{35}$$

$$\rho u_s = -\mathbf{n}\cdot\left(j_{H_2O} + \rho u_s \omega_{H_2O}\boldsymbol{n}\right) \tag{36}$$

E. Modelling Parameters

The physical parameters are chosen as close to the real-world data from the literature as detailed in Table 2. Some assumptions are based on typical default values defined in the Water Electrolyzer Module.

Table 2. PEM electrolyzer – Modelling Parameters

Property	**PEM Electrolyzer**
Electrolyte	Nafion® EW1100 Perfluorosulfonic acid (PFSA) ionomers [2]
Separator	As above [2]
Anode Catalyst (oxygen side)	Platinum + Iridium oxide(IrO_2) [2]
Electrode Catalyst (hydrogen side)	Platinum nanoparticles on carbon black[2]
Porous Transport Layer	Platinized porous titanium (H_2O side)[2]
Gas Diffusion Layer	Sintered porous titanium or carbon felt (H_2 side)[2]
Porosity of Diffusion / Transport Layers	0.3 (assumed)
Pore Volume in Diffusion / Transport Layers	0.6 (assumed)
Bipolar Plates	Pt/Ti | Ag/Ti
Reference Exchange Current Density HER	$1x10^{-3}$ A/cm^2 [9]
Reference Exchange Current Density OER	$1x10^{-7}$ A/cm^2 [9]
Cell Voltage (V_{cell})	1.3–2.2 V

Property	PEM Electrolyzer
Current Density[6]	1-2 A/cm^2 as on date [6],[9],[10]
Cell Temperature	80 ℃
Inlet Pressure at O_2 Side	1.01 bar [9],[10]
Water Inlet Velocity	0.08 m/s @ 3ml/min (assumed based on works of S. Bhaskaran et al[11])
Outlet Pressure at H_2 Side	13.7 bar[9],[10]
Porosity of Diffusion / Transport Layers	0.3 (assumed)
Permeability through Diffusion Layers	1x10^{-8} m^2 (assumed)
Pore Volume in Diffusion / Transport Layers	0.6 (assumed)

All coefficients and properties necessary to model water transport properties through PEM are chosen from the COMSOL Material Library. The COMSOL library offers the properties of Nafion® EW1100 membranes as liquid-equilibrated and vapor-equilibrated variants. The liquid equilibrated membrane properties are considered at the domain level for the primary properties, including electrical conductivity, water transport coefficient, and electroosmotic coefficient.

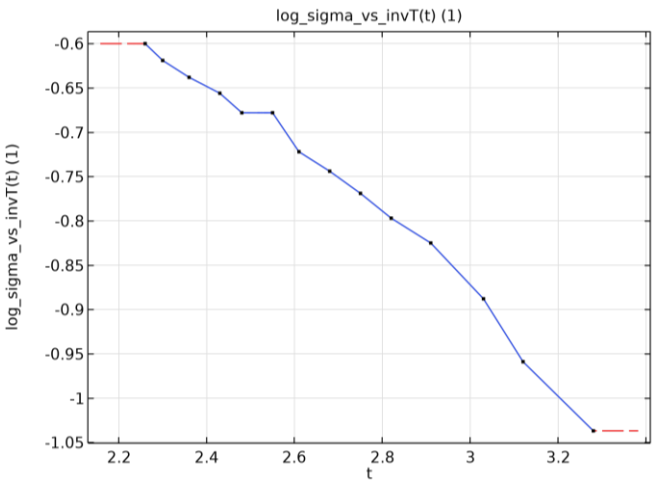

FIG. 7. Empirical function for ion conductivity of PEM in COMSOL 6.3

The electrolyte conductivity for liquid equilibrated PEM is given in the COMSOL Material Library for Nafion® EW1100 based on the work of Robert W. Kopitzke et al[16] using Equation 37.

$$\sigma_{pem} = 10^{f_{\sigma,T}\left(\frac{1000}{T}\right)} \tag{37}$$

The function $f_{\sigma,T}$,is a logarithmic relationship between the log of conductivity, σ expressed in S/m, and the inverse of system temperature, T, expressed in K.

The water transport coefficient, α_{wtc} expressed in s.mol^2/(kg.m^3) considering a liquid equilibrated PEM domain is given as a function of system temperature, T expressed in K in the COMSOL Material Library for Nafion® EW1100 using the Equation 38.

$$\alpha_{wtc} = (3 \times 10^{-6}) \times e^{\left(\frac{14000}{R}\left(\frac{1}{25℃}-\frac{1}{T}\right)\right)} \tag{38}$$

The electroosmotic coefficient ξ for a liquid equilibrated PEM domain is defined based on works of Weber and Neumann[12] as a dimensionless quantity relative the system temperature, T expressed in ℃ in the COMSOL Material Library for Nafion® EW1100 using the Equation 39.

$$\xi = 2.55 \times e^{\left(\frac{4000}{R}\left(\frac{1}{30℃}-\frac{1}{T}\right)\right)} \tag{39}$$

At the H_2 gas (cathode) side, the vapor absorption-desorption rate constants are applied at the boundary level from the Nafion® EW1100 vapor equilibrated membrane definitions from the COMSOL library based on works by B Kientiz et al[17] for a vapor equilibrated membrane. The absorption desorption rate constant $k_{abs,dsp}$ expressed in *mol/(m^2.s)* is predefined and available in the COMSOL Material Library for Nafion® EW1100, given by the Equation 40.

$$k_{abs,dsp} = 0.00104\ e^{4.48 \times a_w} \tag{40}$$

where a_w is the activity of water at the vapor equilibrated membrane surface (not to be confused with thermodynamic activity of water (a_0) [12]). The function is well defined within the interval $0.25 \leq a_w \leq 0.85$ and extrapolated as a constant extending on either side outside the limits.

The inlet water is considered as an incompressible fluid at cell temperature, i.e., 80℃ and 1.01 bar pressure. Under stationary conditions, the fluid is considered a single-phase Darcian flow. The oxygen concentration of high-purity water (deionized water) is assumed to be in the range of 10 ppm. No other species, including N_2, is assumed in water. Hence, the mole fraction of water at the anode inlet ($x_{H_2O,in}$) is set to 0.99999.

The water inlet velocity is assumed to be 3ml/min. Since water is fed in liquid (single) phase through a channel of cross sections defined in Table 1, the velocity is calculated to be 0.078m/s, which exceeds the stoichiometric water

consumption by nearly 223 times based on a typical operating current density of 2 A/cm^2.

The H_2 gas is considered to be recirculated at the rated system pressure (13.7 bar) and assumed to be a damp, humidified mixture at room temperature, i.e., 28 °C (T_{hum}). The saturated vapor pressure of water is dependent on the temperature but relatively less on the absolute pressure. An empirical relationship between the saturated vapor pressure expressed in hPa and the humidification temperature expressed in °C is given by the Arden Buck equation expressed as Equation 41 [9][13].

$$p_{H_2O,sat} = 6.1121\, exp\left(\left(18.678 - \frac{T_{hum}}{234.5}\right)\left(\frac{T_{hum}}{257.14 + T_{hum}}\right)\right) \quad (41)$$

Thus, the initial mole fraction of water in the H_2 recirculation stream can be estimated using the expression for mole fraction relative to absolute pressure given by Equation 42.

$$x_{H_2O|H_2,in} = \frac{p_{H_2O,sat} \times RH}{P_{total}} \quad (42)$$

It is further assumed that the recirculation stream is fully saturated with water vapor, i.e., Relative humidity (RH) is 100% and enters the domain at room temperature ($T_{in} = T_{hum}$ = 28 °C). Thus, the mole fraction of water in the H_2 recirculation inlet is set to 0.0027.

The temperature is set as a common model input through the *default model inputs* node. In contrast, the pressures on the anode and cathode sides are set to differentiate species activity on either side of the Membrane.

VI. RESULTS AND DISCUSSION

The study node is set up such that the model is first solved with an initiation step to evaluate the current distribution based on Ohm's law (primary), followed by a secondary current distribution step taking into account the activation overpotential.

The polarization characteristics of the four different cases are presented along with the experimental data [9],[10]. It is to be noted that, the exact experimental conditions could not be retrieved from the available information, and assumptions have been made about several parameters that influence the overpotentials, including the conductivity and permeability of the porous transport layer at the anode and the gas diffusion layers at the cathode which contribute to significantly to the voltage losses driven by diffusion, convection and migration (mass transport) driven voltage losses. From FIG. 8, it is evident that the reaction kinetics are governed by mass transport characteristics in the water electrolyzer. This is expected for any electrochemical system operating at voltages significantly greater than the equilibrium potential of the system. The application of velocity fields in the model has significantly contributed to the polarization curve in approaching the experimental data. A thin layer of PEM electrolyte reduces the ohmic resistance across the electrodes; however, the diffusion characteristics of the electrode seem to have taken over.

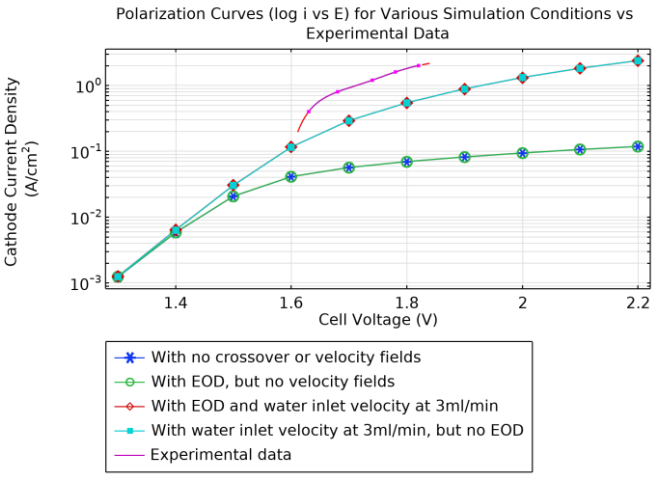

FIG. 8. Polarization characteristics of Water Electrolyzer under different simulation conditions

The electroosmotic water drag apparently has negligible contributions to the polarization characteristics based on observations with respect to the corresponding cases with and without considerations of electroosmotic water drag (EOD). This observation could be different with thicker membranes, which may be considered for operations at higher pressures.

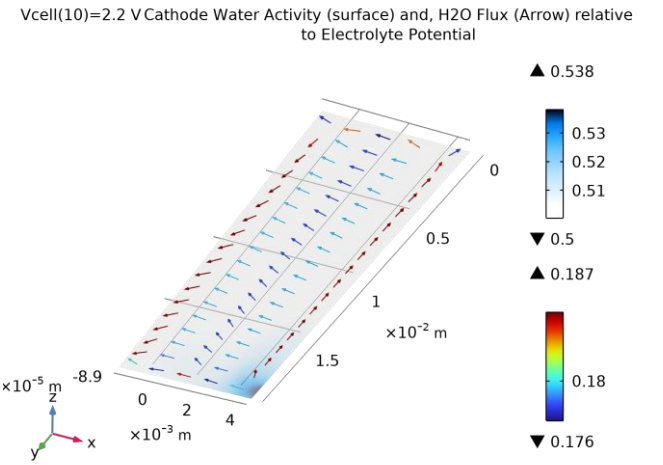

FIG. 9. Water activity (RH) at PEM surface exposed to H2 side at a cell voltage of 2.2V, with water inflow velocity of 3ml/min in the anodic channel, but with no water crossover considerations

It can be seen from FIG. 9 and FIG. 10 that there is significantly higher, i.e., nearly 81% more water activity when water transport through electro-osmotic drag is considered.

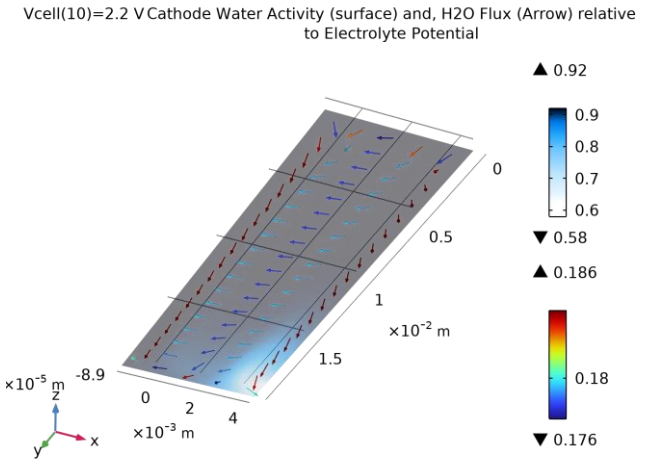

FIG. 10. Water activity (RH) at PEM surface exposed to H2 side at a cell voltage of 2.2V, with water inflow velocity of 3ml/min in the anodic channel under the consideration of water transport through electroosmotic water drag.

From FIG. 11 a subtle influence from the velocity field of water flowing in the anode domain on the water activity of the membrane exposed to the cathode domain can be noticed by the disparity between the green/circle and red/diamond curve, as well as between the blue/asterisk and cyan/square curves.

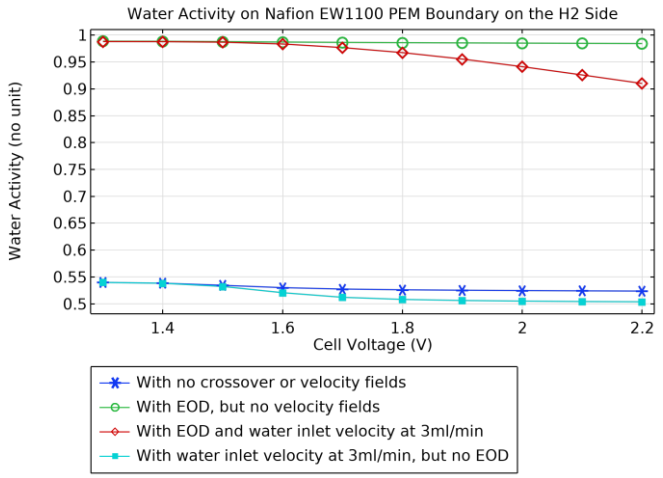

FIG. 11. Variations in water activity (relative humidity) on the cathode side surface of PEM

This is an interesting observation, which can be due to one of the following mechanisms:

a. Accelerated consumption due to entrapment of water along with excessive H_2 gas evolution at the gas diffusion electrode

b. backflow driven by accelerated consumption of water from the PEM electrolyte near the anode surface at high operating current densities, causing a flow of water opposite to the flow associated with H^+ ion movements

The second scenario stated above is not evident in the plots presented as FIG. 9 and FIG. 10, however, water starvation at the anode at high operating current densities is discussed in studies by S. Bhaskaran et al[11].

The water streamlines in the anode and cathode domains in both isometric and profile views are shown in FIG. 12 and FIG. 13 for the case with no water crossover consideration and that with electroosmotic water drag across the membrane, respectively. In both the figure groups, the streamlines corresponding to the residual water present in H_2 recirculation streams are filtered, and *only contributions due to electroosmotic water drag* are made visible by filtering out the initial mole fraction introduced in the model.

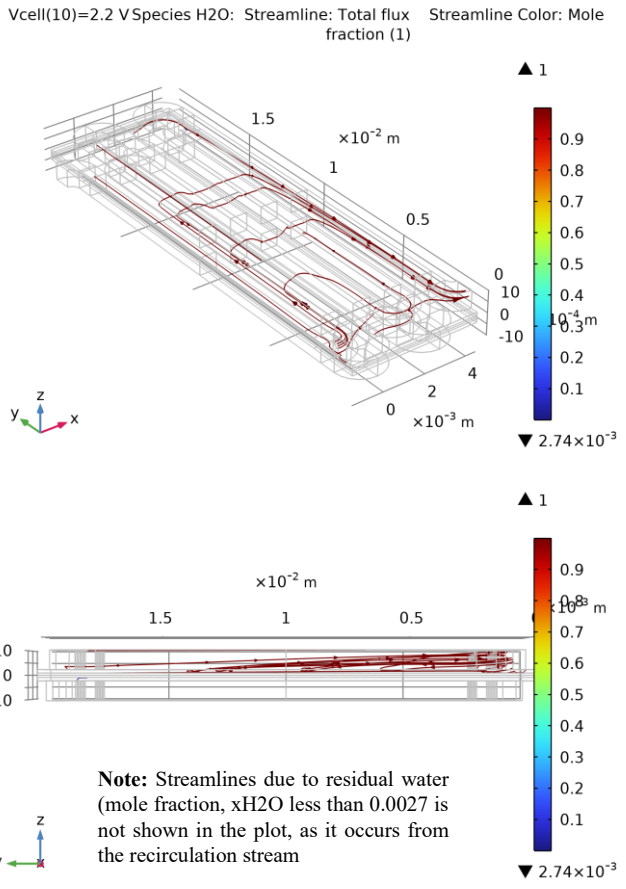

FIG. 12. Water flux through PEM (relative humidity) with a water inlet velocity of 3ml/min at the anode, with no water crossover consideration

It is noticed that the water flows readily through the diffusion layers, similar to the channels in the anode

compartment. This is expected to be a combined effect of porosity, path length, and inflow velocity. It could also be an effect of rapid bubbling due to O_2 gas generation that occurs at high current densities close to 2A/cm^2 [11] at the anode. A similar flow pattern is not seen with the flow occurring at higher pressures in the cathode channels at low flow rates.

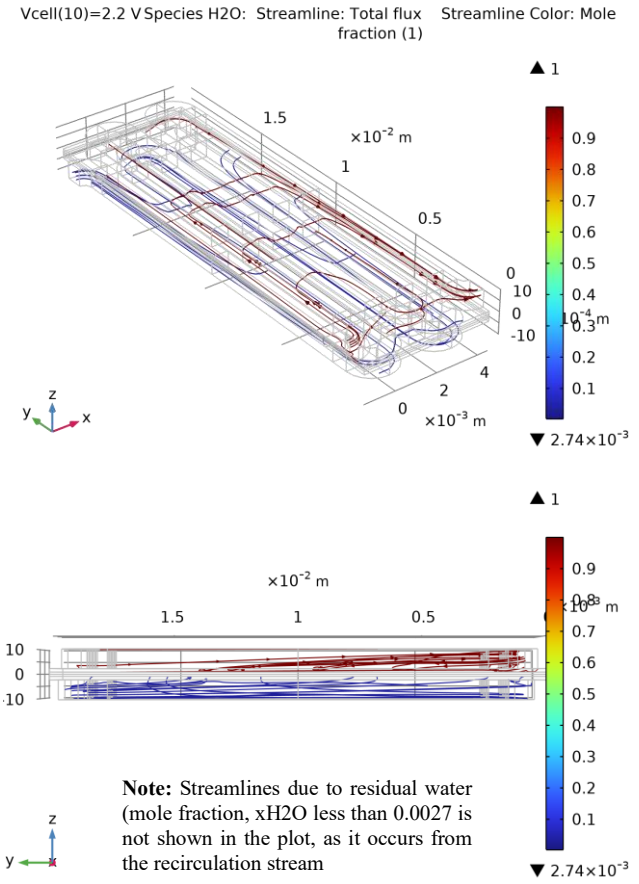

FIG. 13. Water flux through PEM (relative humidity) with a water inlet velocity of 3ml/min at the anode, with consideration to electroosmotic water drag

From FIG. 14 it can be clearly seen that the total water flux through the PEM at the H_2 cathode side of the water electrolyzer increases with the water inflow velocity. With the operating parameters considered, the water flux through the PEM is approximately 3.5x10^{-5} g/s at a Cell voltage of 2.2V, which corresponds to an operating current density of approximately 2.4A/cm^2.

The surface area of the PEM considered in this study is 60 mm^2. Thus, the typical rate of water crossing over to the humid stream at nearly 2.4 A/cm^2 is estimated to be around 0.0035 g/(cm^2·min). This corresponds to nearly 26% of the stoichiometric water consumption at the operating current density of 2.4 A/cm^2 on the anode surface, calculated to be 0.0134 g/(cm^2·min). However, since the volumetric flow rates through the anode chambers are typically higher than the theoretical/stoichiometric water consumption (in the orders of 200 – 1000), this water loss would account for only 0.07% of the water inlet flow rate at 0.078m/s assumed in this model. This could be a misleading factor in the economic analysis and incur unprecedented losses in high-purity water necessary for green H_2 production through electrolysis, requiring means to capture water lost in the H_2 stream and deionize water, potentially resulting in an increased carbon footprint of the process, if not affecting the overall conversion efficiency.

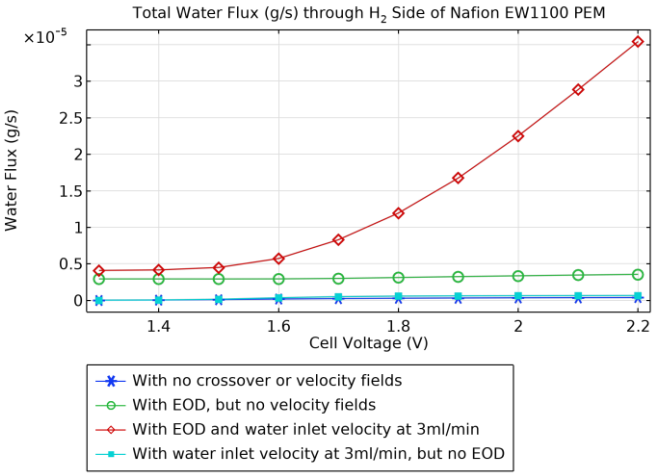

FIG. 14. Variations in water flux through the H_2 side of the PEM surface

V. CONCLUSIONS

Water lost through humid H_2 stream is seen to rise rapidly at cell voltages greater than 1.6 V (corresponding to approximately 0.04 A/cm^2). At cell voltages as high as 2.2 V and approximately 2.4 A/cm^2, the potential water loss can be as high as 0.0035 g/(cm^2·min), which corresponds to nearly 26% of the theoretical water consumption (~0.0134 g/(cm^2·min)) at the said current density. This is expected to go higher with the increase in the operating current densities.

The water flux through the membrane is influenced by the cell voltage and the velocity of water flowing in through the anode channels. A subtle downtrend in water activity on the cathode side of the Nafion membrane is observed when water velocity fields are considered in the anode domain. This may be due to the absorption and desorption of water as a humid stream into the H_2 gas domain and/or rapid conversion of water in the electrolyte due to dissociation at the anode, resulting in a counteracting gradient.

It is a derived learning from this analysis that the transport properties are more significant and essential characteristics that need to be adequately defined for a more realistic simulation of water electrolyzer than the electrochemical parameters, like exchange current density or charge transfer coefficients. This is probably because the electrolyzer operates in the mass transport dominant kinetic region when

operating at voltages greater than 200 mV, more than the reversible voltages.

A low resistivity of the electrolyte between the cathodes and anodes is essential, but may not be sufficient to reduce the power losses. The transport properties of the streams on both sides are to be considered for energy optimization.

Channel dimensions and flow rates are also expected to influence the overall performance of the water electrolyzer, including efficient usage of resources like high-purity water. However, such a study shall be accompanied by more rigorous experimental analysis.

This study serves only as a baseline and needs to be extended further into studying membrane sensitivity related to

- temperature gradients, including the latent heat transfers related to phase change across the membrane
- balanced and unbalanced cell pressures
- turbulent velocities and bubbling
- operations at extreme current densities, which are projected to be reached in the future, say 4-6 A/cm^2 by 2050, with the development of new age catalysts[6]

ACKNOWLEDGMENTS

The authors gratefully acknowledge the technical and academic support of the Multiphysics Modelling School (https://www.multiphysics.uma.es).

REFERENCES

[1] S. S. Kumar, H. Lim, An overview of water electrolysis technologies for green hydrogen production, *Energy Reports*, **Vol. 8** (2022). https://doi.org/10.1016/j.egyr.2022.10.127

[2] IRENA, 2020b. Green Hydrogen Cost Reduction. "Scaling up electrolyzers to meet the 1.5 °C climate goal." International Renewable Energy Agency, Abu Dhabi (2020). ISBN: 978-92-9260-295-6

[3] S. S. Kumar, V. Himabindu, Hydrogen production by PEM water electrolysis – A review, *Mat. Sci. for Energy Technologies* **2**, 3 (2019). https://doi.org/10.1016/j.mset.2019.03.002

[4] R. Hancke, P. Bujlo, T. Holm, Ø. Ulleberg, High-pressure PEM water electrolyzer performance up to 180 bar differential pressure, *J. Power Sources* Vol. **601** (2013). https://doi.org/10.1016/j.jpowsour.2024.234271

[5] G. Correa, P. Marocco, P. Munoz, T. Falaguerra, D. Ferrero, M. Santarelli, Pressurized PEM water electrolysis: Dynamic modeling focusing on the cathode side, *Int. J. Hydrogen Energy* **47**, 7 (2022). https://doi.org/10.1016/j.ijhydene.2021.11.097

[6] Masahiro Yasutake et al., Hybrid Anode Design of Polymer Electrolyte Membrane Water Electrolysis Cells for Ultra-High Current Density Operation with Low Platinum Group Metal Loading, *J. Electrochem. Soc.* **170**, 124507 (2023). https://doi.org/10.1149/1945-7111/ad1165

[7] M. Schalenbach, M. Carmo, D. L. Fritz, J. Mergel, D. Stolten, Pressurized PEM water electrolysis: Efficiency and gas crossover, *Int. J. Hydrogen Energy* **38**, 35 (2013). https://doi.org/10.1016/j.ijhydene.2013.09.013

[8] M. Schalenbach, Corrigendum to "Pressurized PEM water electrolysis: Efficiency and gas crossover" [Int J Hydrogen Energy 38 (2013) 14921-14933], *Int. J. Hydrogen Energy* **41**, 1 (2016). https://doi.org/10.1016/j.ijhydene.2015.11.009

[9] A. S. Tijani et al., Electrochemical characteristics of (PEM) electrolyzer under the influence of charge transfer coefficient, *Int. J. Hydrogen Energy* **44**, 50 (2019). https://doi.org/10.1016/j.ijhydene.2019.08.188

[10] M. K. Debe et al., Initial Performance and Durability of Ultra-Low Loaded NSTF Electrodes for PEM Electrolyzers, *J. Electrochem. Soc.* **159**, 6 (2012). https://doi.org/10.1149/2.065206jes

[11] S. Bhaskaran et al., Model PEM water electrolyzer cell for studies of periodically alternating drainage/imbibition cycles, Int. J. Hydrogen Energy **77** (2024). https://doi.org/10.1016/j.ijhydene.2024.06.268

[12] A. Z. Weber, J. Newmann, Transport in Polymer-Electrolyte Membranes II. Mathematical Model, *J. Electrochem. Soc.* **151**, 2 (2004).

[13] https://en.wikipedia.org/wiki/Arden_Buck_equation

[14] M. Carmo, D. L. Fritz, J. Mergel, D. Stolten, A comprehensive review on PEM water electrolysis, *Int. J. Hydrogen Energy* **38**, 12 (2013). https://doi.org/10.1016/j.ijhydene.2013.01.151

[15] A. Benmehel, T. Kouksou, et al., PEM water electrolyzer modeling: Issues and reflections, *Energy Conversion and Management: X* 24 (2024). https://doi.org/10.1016/j.ecmx.2024.100738

[16] R. W. Kopitzke, C. A. Linkous, H. R. Anderson and G. L. Nelson, Conductivity and Water Uptake of Aromatic-Based Proton Exchange Membrane Electrolytes, *J. Electrochem. Soc.* **147**, 5 (2000). https://doi.org/10.1149/1.1393417

[17] B. Kientiz, H. Yamada, N. Nonoyama, A. Z. Weber, Interfacial Water Transport Effects in Proton-Exchange Membranes, *J. Fuel Cell Sci. Technol.* **8**, 1 (2011). https://doi.org/10.1115/1.4002398

[18] N. Lin, J. Zausch, 1D multiphysics modeling of PEM water electrolysis anodes with porous transport layers and the Membrane, *Chemical Engineering Science* **253** (2022). https://doi.org/10.1016/j.ces.2022.117600

[19] COMSOL, Fuel Cell and Electrolyzer Module User's Guide, Version COMSOL 6.3 (2023).